



Universiteit  
Leiden  
The Netherlands

## Structure dependence of molecular reactions on surfaces

Cao, K.

### Citation

Cao, K. (2018, October 11). *Structure dependence of molecular reactions on surfaces*. Retrieved from <https://hdl.handle.net/1887/66120>

Version: Not Applicable (or Unknown)

License: [Licence agreement concerning inclusion of doctoral thesis in the Institutional Repository of the University of Leiden](#)

Downloaded from: <https://hdl.handle.net/1887/66120>

**Note:** To cite this publication please use the final published version (if applicable).

Cover Page



Universiteit Leiden



The handle <http://hdl.handle.net/1887/66120> holds various files of this Leiden University dissertation.

**Author:** Cao, K.

**Title:** Structure dependence of molecular reactions on surfaces

**Issue Date:** 2018-10-11

## Chapter 3

# A molecular beam study of $D_2$ dissociation on Pt(111): testing SRP-DFT calculations

### 3.1 Introduction

The interaction between  $H_2$  or  $D_2$  with Pt surfaces has been a model system for dissociative chemisorption for a long time [18, 19]. In experiments scattering and diffraction, rotational excitation and selective adsorption, and dissociative adsorption (or sticking) have been studied[20–25]. In this study we focus on dissociative chemisorption at high energies of 0.1 to 0.5 eV on Pt(111). Not only on the close packed Pt(111) surface but also on stepped Pt surfaces hydrogen dissociation has been studied recently in detail[26–30]. The step edge introduces additional mechanism for adsorption near the step edge, that are irrelevant for the present study[31, 32].

Over the years theoretical studies have been carried out with increasing sophistication. The Born-Oppenheimer Approximation has been demonstrated to work under these conditions[33–35]. This allows the separate calculation of a potential energy surface (PES) and dynamics calculations using a given PES. For adsorption studies, it is relevant to mention that the dimensionality of the calculations has increased over the years, from 2D (internuclear distance of  $H_2$  and molecule surface separation assuming a structureless surface) to 6D: 3

intramolecular degrees of freedom and the 3D position of the molecule above the surface[36, 37]. Both quantum mechanical and classical calculations have been used to compute sticking coefficients[38].

Although in the past empirical PES have been used, recently the PES is computed by Density Functional Theory (DFT). The results show that the PES is elbow type and has an early barrier [36, 39]. The barrier height strongly depends on the lateral position of the molecule above the surface and the molecular orientation. Most recent calculations show that the barrier height can be as low as -0.008 eV on the top site to almost 0.5 eV on the hcp adsorption site[39]. This implies that adsorption can be barrier less, but because most surface sites show a small barrier towards sticking the system overall exhibits weakly activated sticking. Since the barrier height is site dependent, the PES shows energetic corrugation. In addition, the distance between the molecule and the surface at the barrier is also site dependent: thus, the PES also shows geometric corrugation. These terms have been introduced by Darling and Holloway[40, 41]. In general, strong energetic corrugation leads to a reduction of sticking with increasing parallel momentum, for constant normal energy  $E_n = E_i \cos^2(\Theta_i)$ , where  $\Theta_i$  is the incidence angle measured from the surface normal and  $E_i$  the beam energy. In contrast, strong geometric corrugation leads to an increase in sticking with increasing parallel momentum. The most recent theoretical calculations for this system have been carried out in the Kroes group, see[39]. Pijper et al. observe that their PES shows both energetic and geometric corrugation [36].

The group of Kroes proposed to allow an adjustable Specific Reaction Parameter (SRP) in the DFT functionals used, to obtain chemical accuracy in the DFT calculations and obtain good agreement between theory and experiment for several different observables[34, 42]. The method has been calibrated by Ghassemi et al. on normal incidence sticking data of D<sub>2</sub> on Pt(111) by Luntz et al[22]. The resulting SRP-DFT PES was tested on Luntz's data for non-normal incidence. The agreement between theory and experiment was very good, indicating that the SRP-DFT potential is very good. However, Luntz et al. did not specify the azimuthal orientation of the crystal with respect to the incidence plane of the beam. So the dependence of sticking on the azimuthal orientation of the crystal should be determined experimentally. The two most important orientations of the incidence plane ( $\Phi$ ) are  $[10\bar{1}]$  and  $[11\bar{2}]$ , corresponding here to  $\Phi = 30^\circ$  and  $\Phi = 0^\circ$  The

theoretical prediction by Ghassemi et al. is that the differences will be very small, except at  $\Theta_i = 60^\circ$ [39]. It is the aim of this paper to experimentally test the theoretical prediction and determine the azimuthal dependence of  $D_2$  sticking on Pt(111).

## 3.2 Experimental

Experimental methods and our UHV-molecular beam system have been described before[30, 43–45]. Briefly, a triply differentially pumped molecular beam is aimed at the polished and cleaned (111) surface of a 10 mm diameter, 1 mm thick Pt single crystal kept in an ultrahigh vacuum (UHV) chamber. The energy of the molecular beam can be varied by heating the nozzle and by seeding  $D_2$  in  $H_2$  or inert gases, e.g. Ne,  $N_2$  and Ar. An inline quadrupole mass spectrometer (QMS) with a cross-beam ionizer detects molecules in the beam. Using time-of-flight (TOF) techniques and a mechanical chopper, TOF spectra of the beam can be obtained. The distance between the chopper wheel and the ionizer can be adjusted continuously over 200 mm, to allow accurate determination of the offsets and delays in the flight time. We fit the TOF spectra in the time domain and represent the fit in the energy domain to extract the most probable energy and energy spread in the beam. From this data, we calculate the average energy,  $E_{avg}$ , of our beams when comparing to data from previous studies.

The Pt(111) surface is prepared with a mis-cut angle of less than  $0.1^\circ$  (Surface Preparation Laboratory, Zaandam, the Netherlands). It is cleaned daily by multiple sputtering, oxidation, reduction, and annealing cycles. We sputter at 600 eV with  $\sim 2.5\mu A$   $Ar^+$  current during 5 minutes at a surface temperature,  $T_S$ , of 900 K. This is followed by a mild oxidation at the same surface temperature (2 minutes,  $p(O_2) = 2 \times 10^{-7}$  mbar),  $H_2$  reduction at the same surface temperature (2 minutes,  $p(H_2) = 2 \times 10^{-6}$  mbar) and annealing at 1200 K for 5 minutes. Surface order is regularly verified by low energy electron diffraction (LEED, OCI Vacuum, BDL800IR-MCP) and cleanliness by Auger Electron Spectroscopy (AES, Staib Instruments DESA).

Sticking coefficients are obtained using the method of King and Wells (KW)[10]. We remove background signal from residual hydrogen prior to opening the UHV chamber to the differential stages of the supersonic molecular beam. We normalize the signal from the

molecular beam when it is admitted to the UHV chamber. We then inverting the time-dependent KW trace and fit the time-dependent reaction probability by a double exponential functional form starting at approx. 0.5–1.0 s after opening the beam flag. We extrapolate the fit backward to the exact time of opening this last flag and obtain the reaction probability from the fit. This procedure removes the convolution of the signal with the time required to fully remove the beam flag and the vacuum time constant of the UHV chamber for molecular hydrogen. The reported experimental error in the initial sticking coefficient is one standard deviation determined from repeating measurements under identical conditions.

## 3

### 3.3 Results and discussion

In Figure 3.1 the results for normal incidence are shown for  $T_S = 200$  K. Our data are in good agreement with previous experiments by Luntz et al. and Samson et al. [21, 22]. In addition, we present results for two well-defined azimuthal orientations of the crystal. We note that there is very little difference between  $\Phi = 0^\circ$  and  $\Phi = 30^\circ$ . This is to be expected as for normal incidence the sticking should be independent of  $\Phi$ . The small differences observed should be due to imperfections of the crystal or the beam alignment. Our data for  $\Phi = 0^\circ$  and  $\Phi = 30^\circ$  indeed are the same within experimental error. The lines drawn through our data are quadratic fits and shown to guide the eye only. As discussed before, agreement between theory and experiment is very good, because the data by Luntz et al. were used to calibrate the SPR-DFT PES.

In Figure 3.2 data for off-normal incidence are presented, also for  $T_S = 200$  K. Our data at  $\Theta = 30^\circ$  and both  $\Phi$  values are in good agreement with the data of Luntz. The data for both  $\Phi$  values are the same within experimental error. Only above 0.37 eV do we find that Luntz’s data are slightly higher than ours. A source of discrepancy for high nozzle temperature H<sub>2</sub> (D<sub>2</sub>) molecular beams may be differences in the energy dispersion, causing variation in the convolution with the energy-resolved sticking probability[34]. The theory of Ghassemi et al.[39] follows Luntz’s data. Our data at  $\Theta = 40^\circ$  and both  $\Phi$  values are in good agreement with the data of Luntz for  $\Theta = 45^\circ$ . Our data at  $\Theta = 50^\circ$  and both  $\Phi$  values fall in between the data of Luntz

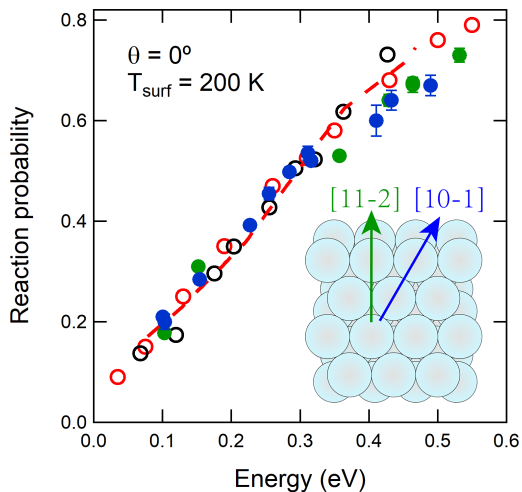


**Figure 3.1:** Energy dependence of the dissociative reaction probabilities of  $D_2$  on Pt(111). Solid circles are our data, the color indicating the azimuthal directions as shown in the inset. The black and red open circles are the experimental data from Samson et al.[21] and Luntz et al.[22], respectively. The red dashed line reproduces the results of dynamical calculation from Ghassemi et al.[39]. Represented energies are the averages of energy distributions calculated from TOF distributions. Error bars indicate one standard deviation for repeated measurements. For single measurements, no error bar is shown.

for  $\Theta = 45^\circ$  and  $\Theta = 60^\circ$ . Because of the different  $\Theta$  values, direct comparison is not possible. The Luntz's data again seem slightly higher than ours at energies above 0.35 eV. The lines drawn through our data are again quadratic fits to guide the eye.

At  $\Theta = 50^\circ$ , the data in Figure 3.2 suggest a slight difference for sticking at  $\Phi = 0^\circ$  and  $\Phi = 30^\circ$ . The resulting sticking curves are shown with an expanded scale in Figure 3.3. At  $\Theta = 50^\circ$ , the difference between  $\Phi = 30^\circ$  and  $\Phi = 0^\circ$  is small with sticking at  $\Phi = 30^\circ$  being slightly higher. With barrier heights being equal, this implies a slightly different geometrical corrugation felt by trajectories along the two different azimuths.

The PES shows that there is an almost complete absence of a precursor well[39]. The average well depth for physisorption is 0.072 eV[39]. This implies that precursor-mediated dissociative adsorption is not possible at  $T_S = 200$  K. This is qualitatively confirmed by the work of Poelsema et al. where only at 25 K significant adsorption is observed [20]. The absence of a deep well also implies that there is no

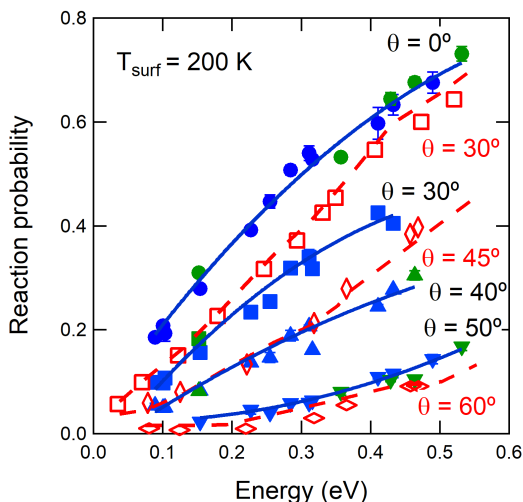


**Figure 3.2:** The dissociative reaction probability dependence on kinetic energy for various polar and azimuthal angles. The solid symbols are our data. Polar angles are indicated by the black text. The color of the solid symbol indicates the azimuthal angle as in figure 3.1. The solid lines are quadratic fits to guide the eye. The open symbols reproduce the experimental data from Luntz et al.[22]. The dashed lines reproduce results of dynamical calculations from Ghassemi et al.[39]. The red text indicates their polar angles.

$T_S$  dependence of the sticking probability. This is confirmed by the data presented in Figure 3.4. No significant  $T_S$  dependence is seen. In addition, in the sticking curves as a function of energy no evidence of the presence of a precursor state is seen. This is also in agreement with the studies of Gee et al., and Groot et al. for stepped Pt(111) surfaces[26, 28–30]. These authors observed significant sticking at low beam energies, that decreases with increasing beam energy. This was attributed to the presence of a deeper molecular chemisorption well near the step edge.

### 3.4 Conclusion

There is excellent agreement between our data and earlier experimental work. Our work demonstrates that the interaction only weakly depends on the azimuthal orientation of the incidence plane. Our data is entirely consistent with the SRP-DFT calculations on D<sub>2</sub> on Pt by Ghassemi et al[39]. It demonstrates that the SRP-DFT methodology

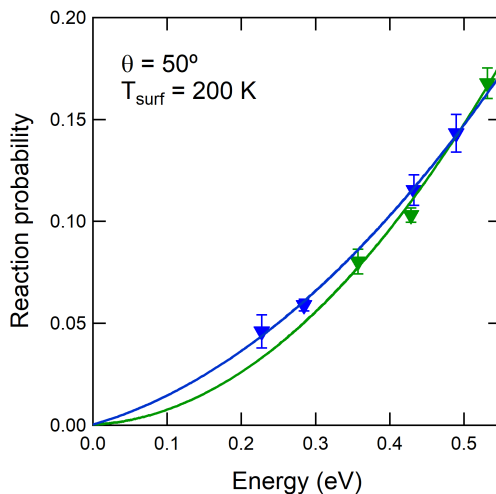


**Figure 3.3:** Reaction probabilities versus kinetic energy at  $50^\circ$  polar angle for both azimuthal angles. Colors for the azimuthal angle are used as in figures 3.1 and 3.2. Error bars are standard deviation determined from multiple measurements at identical conditions.

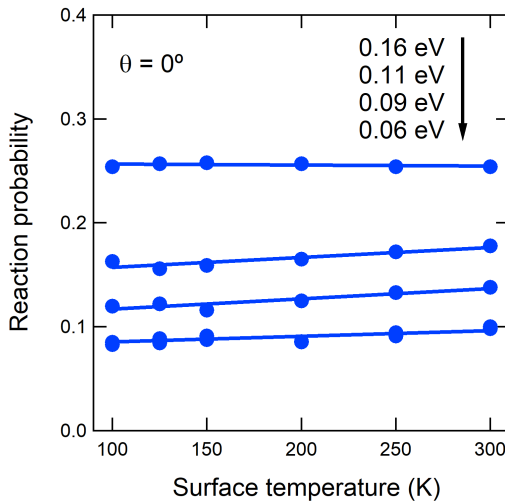


**Figure 3.4:** The surface temperature dependence of the dissociative reaction probability on Pt(111) for incident energies as indicated in the figure.

works for this system at the level of the azimuthal dependence of the sticking probability for non-normally incident beams. There are possibly small discrepancies at large polar incidence angles and high energies. More detailed, focused experiments and calculations are needed

to investigate if there is a significant difference between theory and experiment for those special conditions.